The 2009 IEEE/RSJ International Conference on
Intelligent Robots and Systems
October 11-15, 2009 St. Louis, USA

Dynamic Modeling for Locomotion-manipulation of a Snake-like Robot by Using Geometric Methods

Zhifeng Wang, Shugen Ma, Bin Li, and Yuechao Wang

***Abstract*— A snake-like robot can locomote in various environments; and it can manipulate objects when one end is fixed. A method of dynamic modeling for locomotion-manipulation of the snake-like robot is developed in order to unify the dynamic equations of two states. A virtual structure for orientation and position and the product-of-exponentials formula describe the mechanism and the kinematics of the robot. The dynamics of the robot are established in a Riemannian manifold. Furthermore, the dynamics of manipulation can be directly degenerated from those of locomotion. This method unifies the dynamics of locomotion and manipulation of the snake-like robot in the differential geometry formulation. Finally, simulation results of the method are presented.**

I. Introduction

Imitating the body of a snake, the structure of a snake-like robot is an articulated mechanism without a fixed base. The snake-like robot can widely adapt to various environments. On the other hand, the snake-like robot is a redundant manipulator, if one end is fixed on a base. Integrating locomotion and manipulation makes the robot powerful in many fields, such as searching and rescuing in disasters, inspecting and repairing in industries.

In the last decade, many scholars were interested in the snake-like robot, especially the dynamics of the robot. Hirose took a bio-mimetic approach in researching the snake-like robot and presented the serpenoid curve of the snake's body [1]. Ostrowski and Burdick discussed the snake-like robot locomotion theory based on geometric mechanics [2]. Ma developed the dynamics model by applying the Newton-Euler method [3]. Saito *et al.* decoupled the dynamics of the robot and determined the feedback control architecture [4]. Liljebäck *et al.* first considered the snake-like robot as a manipulator with a virtual structure for orientation and position (VSOP) [5]. In addition, Andersson approximated a continuous curve with the snake-like robot based on the product-of-exponentials (POE) formula [6].

Because of complexity, those researches studied the dynamics of locomotion and manipulation not unitedly but separately. In fact, the mechanism of the locomotor and that of the manipulator are articulated multi-link systems, and this similarity must lead to some interesting relationships of dynamics essentially. Based on this motivation, the dynamic equations for locomotion and manipulation of the snake-like robot are unified by taking advantage of a geometrical formulation. In the process of unifying and comparing, the unified dynamics offer insight beyond the separate ones. For example, some particular dynamic structure of the snake-like robot are revealed in the unified model.

This work is supported by the Knowledge Innovation Program of Chinese Academy of Sciences 07A1200101 and the National High Technology Research and Development Program of China (863 Program) 2006AA04Z254.

Z. Wang is with State Key Laboratory of Robotics, Shenyang Institute of Automation, Chinese Academy of Sciences, Shenyang 110016, China. He is also with Graduate University of Chinese Academy of Sciences, Beijing 100039, China zfwang@sia.cn

S. Ma is with the Department of Robotics, Ritsumeikan University, Shiga-ken 525-8577, Japan. He is also with State Key Laboratory of Robotics, Shenyang Institute of Automation, Chinese Academy of Sciences, Shenyang 110016, China shugen@se.ritsumei.ac.jp

B. Li and Y. Wang are with State Key Laboratory of Robotics, Shenyang Institute of Automation, Chinese Academy of Sciences, Shenyang 110016, China libin@sia.cn; ycwang@sia.cn

II. Kinematics of a Snake-like Robot

A. Configuration Description

The snake-like robot can move in various environments; and it can manipulate with fixing one end on a base. The configuration space of locomotion (Q) is divided into a fiber space (G), which describes the position and orientation, and a base space (N), which represents the shape of the robot [2]; that is, $Q = G \times N$. The configuration in coordinates can be written as

$$x = \left[x^1, \ldots, x^n\right]^{\mathrm{T}} \in Q.$$

The motors control the joint angles ($[x^4, \ldots, x^n]^{\mathrm{T}} \in N$) in order to move the position and orientation of the robot on a plane ($[x^1, x^2, x^3]^{\mathrm{T}} \in G$). When the snake-like robot is in a manipulation situation, no change happens in the position and orientation. In other words, the configuration in the manipulation situation is a submanifold of Q, which is denoted by Q', and in coordinates

$$x' = \left[0, 0, 0, x^4, \ldots, x^n\right]^{\mathrm{T}} \in Q'.$$

Whereas, the configuration of the snake-like manipulator is the joint space N, and in coordinates

$$x'' = \left[x^4, \ldots, x^n\right]^{\mathrm{T}} \in N.$$

We use the VSOP method considering the move in the direction of X and Y and the turn around the Z axis as the virtual joint movements with respect to the inertial coordinate frame (Fig. 1). Accordingly, the snake-like robot (locomotion and manipulation) and the manipulator (manipulation) are regarded as manipulators. Additionally, we should point out that the configuration space of the snake-like robot will not be considered as a total space of a fiber bundle but an ordinary manifold. The mathematical relations of the configurations are depicted in Fig. 2. Explicitly,

$$\alpha : N \to Q', \quad \beta : N \to Q$$

are an embedding and an immersion respectively.

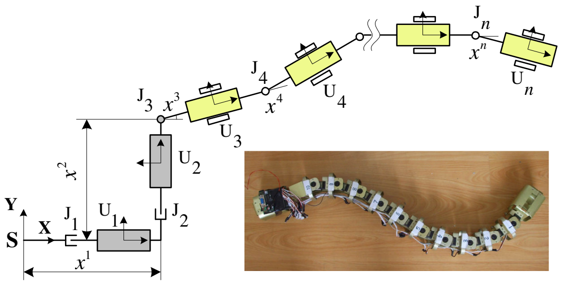

Fig. 1. Model of a snake-like robot

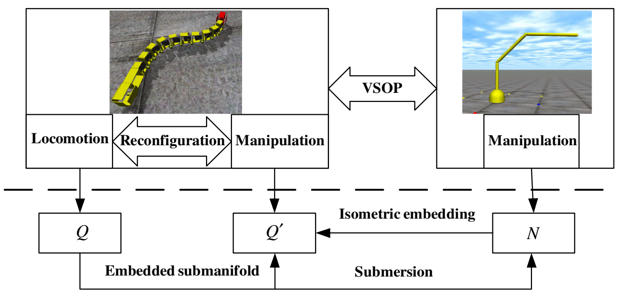

Fig. 2. Mathematical relationships of the configurations

B. Kinematic Formulation

In Fig. 1, U$_1$ and U$_2$ are virtual modules, and the lengths of them are zeros. A real module is denoted by U$_i$, and the length is L_i $(i = 3, \ldots, n)$. We define an inertial coordinate frame S, and set up a module coordinate frame on the geometrical center of each module. The initialization of the joints are zeros. Thus, at the initial moment, the tail of the snake-like robot (J$_3$) is coincident with the origin of the global coordinate system. The configuration of the ith local module frame in S is described by POE ([7]) as follows:

$$g_{s,i} = e^{\hat{\xi}_1 x^1} e^{\hat{\xi}_2 x^2} \cdots e^{\hat{\xi}_i x^i} g_{s,i}(0) = \begin{bmatrix} R_{s,i} & b_{s,i} \\ 0 & 1 \end{bmatrix} \quad (1)$$

for $i = 1, \ldots, n$, where $g_{s,i}(0)$ is configuration of the ith local module frame at the initial moment, x^i short for $x^i(t)$ is the angle (or displacement) variable of the hinge (or prismatic) joint, and $\hat{\xi}_i \in se(3)$ is called a twist describing the screw of the joint.

The configuration space of each module is $SE(3)$, then the extended forward kinematics map of the snake-like robot is

$$\begin{aligned} \kappa : Q &\rightarrow SE^n(3) \\ x &\mapsto (g_{s,1}, g_{s,2}, \ldots, g_{s,n}) \end{aligned}$$

where $SE^n(3)$ is called the Cartesian space [8].

The body velocity of the ith module is denoted by $V_{s,i}^b$,

$$\hat{V}_{s,i}^b = g_{s,i}^{-1} \dot{g}_{s,i}. \quad (2)$$

Therefore, we can get the relation between the angle rates and the body velocity by

$$V_{s,i}^b = J_{s,i}^b(x)\dot{x} \quad (3)$$

where $J_{s,i}^b(x) = [\xi_{i,1}(x), \ldots, \xi_{i,i}(x), 0, \ldots, 0]$ is a $6 \times n$ body manipulator Jacobian matrix [7], and the jth $(1 \leq j \leq i)$ column is

$$\xi_{i,j} = \mathrm{Ad}^{-1}_{\exp(\hat{\xi}_{j+1} x^{j+1}) \cdots \exp(\hat{\xi}_i x^i) g_{s,i}(0)} \xi_j \quad (4)$$

where "Ad" is the adjoint representation of a Lie group. Otherwise, by calculating $e^{-\hat{\xi}_2 x^2} \hat{\xi}_1 e^{\hat{\xi}_2 x^2}$, we know that $\xi_{i,j}$ is independent of x^1 and x^2. Hence, $\xi_{i,j}$ is only dependent on $(x^l, \ldots, x^i)$ where $l = \max\{j+1, 3\}$.

Similarly, the spatial velocity of the ith module

$$V_{s,i}^s = J_{s,i}^s(x)\dot{x} \quad (5)$$

where $J_{s,i}^s(x) = [\xi_{s,1}(x), \ldots, \xi_{s,i}(x), 0, \ldots, 0]$ is a $6 \times n$ spatial manipulator Jacobian matrix [7], and

$$\xi_{s,j} = \mathrm{Ad}_{\exp(\hat{\xi}_1 x^1) \cdots \exp(\hat{\xi}_{j-1} x^{j-1})} \xi_j. \quad (6)$$

III. Dynamics of a Snake-like Robot

We use some geometry conceptions to establish the dynamic equations for locomotion-manipulation. The dynamic equation in the configuration manifold is as follows [8], [9]:

$$\nabla_{\dot{x}} \dot{x} = -\mathrm{grad} V(x) + M^{-1} Y \quad (7)$$

where M, ∇, V, and Y are a Riemannian metric, a Levi-Civita connection, gravitational potential energy, and generalized forces respectively. Locomotion and manipulation of the robot are supposed in a horizontal plane; thus the gravitational potential energy $V(x) = 0$.

A. Riemannian Metric

The Riemannian metric M in the configuration manifold Q is defined with the kinetic energy of the system. A generalized inertia matrix of the ith module in the local coordinate frame can be written as

$$M_i^b = \begin{bmatrix} I_i^b & 0 \\ 0 & m_i E \end{bmatrix}$$

where I_i^b and m_i are the inertia tensor and the mass of the ith module respectively, and E is a 3×3 identity matrix. According to a definition in [5], a virtual joint and module has no mass or inertia, and never exerts any forces or torques, so $M_1^b = M_2^b = 0_{6\times 6}$. The kinetic energy of the system is

$$T = \sum_{i=1}^n T_i = \frac{1}{2} \dot{x}^T \left\{ \sum_{i=1}^n \left(J_{s,i}^b(x)\right)^{\mathrm{T}} M_i^b J_{s,i}^b(x) \right\} \dot{x}. \quad (8)$$

The Riemannian metric in the configuration manifold is not only a $n \times n$ matrix but also a tensor of type $T_2^0(Q)$, and can be presented as

$$M = \sum_{i=1}^n \left(J_{s,i}^b(x)\right)^{\mathrm{T}} M_i^b J_{s,i}^b(x). \quad (9)$$

The metric matrix can be considered as a generalized inertia matrix of the whole system, and the matrix element of M is denoted by M_{ij}, which can be computed as

$$M_{ij} = \sum_{k \geq \max\{i,j\}}^n \xi_{k,i}^{\mathrm{T}} M_k^b \xi_{k,j}. \quad (10)$$

TABLE I

RIEMANNIAN METRIC

	j: 1	2	3
i = 1	$\sum\limits_{i=3}^{n} m_i$	0	$-\sum\limits_{i=3}^{n}\left\{\frac{1}{2}m_iL_i\sin\left(\sum\limits_{j=3}^{i}x^j\right)+m_i\sum\limits_{k=3}^{i-1}\left[L_k\sin\left(\sum\limits_{j=3}^{k}x^j\right)\right]\right\}$
2	0	$\sum\limits_{i=3}^{n} m_i$	$\sum\limits_{i=3}^{n}\left\{\frac{1}{2}m_iL_i\cos\left(\sum\limits_{j=3}^{i}x^j\right)+m_i\sum\limits_{k=3}^{i-1}\left[L_k\cos\left(\sum\limits_{j=3}^{k}x^j\right)\right]\right\}$
3	$\times$	$\times$	$\sum\limits_{i=3}^{n}\left\{\begin{array}{l} I_i^b+\frac{1}{4}m_iL_i^2+m_i\sum\limits_{k=3}^{i-1}L_k^2+ \\ m_iL_i\sum\limits_{k=3}^{i-1}\left[L_k\cos\left(\sum\limits_{j=k+1}^{i}x^j\right)\right]+ \\ 2m_i\sum\limits_{k=3}^{i-2}\sum\limits_{p=k+1}^{i-1}\left[L_kL_p\cos\left(\sum\limits_{j=k+1}^{p}x^j\right)\right] \end{array}\right\}$

Some elements denoted by $\times$ equal the diagonal counterparts because of diagonal symmetry.

From (4) and (10), we know that M_{ij} is a function of the set $(x^l, \ldots, x^n)$ where $l = \min\{\max\{i+1, 3\}, \max\{j+1, 3\}\}$.

Through analysis, we have the following conclusions:

Conclusion 1.1. The partial result of M is shown in Table I, when $i, j = 1, 2, 3$. M is a symmetric positive definite matrix, so (Q, M) is a Riemannian manifold.

Conclusion 1.2. M_{ij} only has relationships with x^k where $k \geq \min\{\max\{i+1, 3\}, \max\{j+1, 3\}\}$, that is, M_{ij} has no relationship with x^1 and x^2, and M_{ij} $(i, j \geq 4)$ is independent of x^1, x^2, and x^3.

B. Levi-Civita Connection

∇ is the Levi-Civita connection of the configuration space, and $\nabla_{\dot{x}}\dot{x}$ is a covariant derivative, which can computed as

$$\nabla_{\dot{x}}\dot{x} = \sum_{i=1}^{n}\left(\ddot{x}^i + \sum_{j,k=1}^{n}\Gamma^i_{jk}\dot{x}^j\dot{x}^k\right)\frac{\partial}{\partial x^i} \tag{11}$$

where Γ^i_{jk} is the Christoffel symbol of the second kind, while Γ_{ljk} describes the Christoffel symbol of the first kind. They have the relationship as

$$\Gamma_{jkl} = \sum_{i=1}^{n} M_{li}\Gamma^i_{jk}. \tag{12}$$

The Christoffel symbol of the first kind is defined as

$$\Gamma_{ijk} = \frac{1}{2}\left(\frac{\partial M_{kj}}{\partial x^i} + \frac{\partial M_{ki}}{\partial x^j} - \frac{\partial M_{ij}}{\partial x^k}\right) \tag{13}$$

and $\Gamma_{ijk} = \Gamma_{jik}$, for $i, j, k = 1, \ldots, n$.

In [10], Park *et al.* presented the equations for computing Γ_{ijk} by using Lie algebra, which are recomposed as follows:

☐ For $k \leq i \leq j$,

$$\begin{aligned}\Gamma_{ijk} = \frac{1}{2}\sum_{l=j}^{n}\Bigg\{&\left(\mathrm{Ad}_l^i\left(\mathrm{ad}_{\hat{\xi}_{i-1,k}}\hat{\xi}_i\right)\right)^{\vee\mathrm{T}} M_l^{\mathrm{b}}\xi_{l,j} \\ &+\left(\mathrm{Ad}_l^j\left(\mathrm{ad}_{\hat{\xi}_{j-1,k}}\hat{\xi}_j\right)\right)^{\vee\mathrm{T}} M_l^{\mathrm{b}}\xi_{l,i} \\ &+\left(\mathrm{Ad}_l^j\left(\mathrm{ad}_{\hat{\xi}_{j-1,i}}\hat{\xi}_j\right)\right)^{\vee\mathrm{T}} M_l^{\mathrm{b}}\xi_{l,k}\Bigg\}\end{aligned} \tag{14}$$

TABLE II

CHRISTOFFEL SYMBOLS OF THE FIRST KIND

k	1									2									3								
i	1			2			3			1			2			3			1			2			3		
j	1	2	3	1	2	3	1	2	3	1	2	3	1	2	3	1	2	3	1	2	3	1	2	3	1	2	3
Γ_{ijk}	0	0	0	0	0	0	0	0	✓	0	0	0	0	0	0	0	0	✓	0	0	0	0	0	0	0	0	0

'✓' means $\Gamma_{ijk} \neq 0$.

☐ For $i < k \leq j$,

$$\begin{aligned}\Gamma_{ijk} = \frac{1}{2}\sum_{l=j}^{n}\Bigg\{&\left(\mathrm{Ad}_l^j\left(\mathrm{ad}_{\hat{\xi}_{j-1,k}}\hat{\xi}_j\right)\right)^{\vee\mathrm{T}} M_l^{\mathrm{b}}\xi_{l,i} \\ &+\left(\mathrm{Ad}_l^j\left(\mathrm{ad}_{\hat{\xi}_{j-1,i}}\hat{\xi}_j\right)\right)^{\vee\mathrm{T}} M_l^{\mathrm{b}}\xi_{l,k} \\ &-\left(\mathrm{Ad}_l^k\left(\mathrm{ad}_{\hat{\xi}_{k-1,i}}\hat{\xi}_k\right)\right)^{\vee\mathrm{T}} M_l^{\mathrm{b}}\xi_{l,j}\Bigg\}\end{aligned} \tag{15}$$

☐ For $i \leq j < k$,

$$\begin{aligned}\Gamma_{ijk} = \frac{1}{2}\sum_{l=k}^{n}\Bigg\{&\left(\mathrm{Ad}_l^j\left(\mathrm{ad}_{\hat{\xi}_{j-1,i}}\hat{\xi}_j\right)\right)^{\vee\mathrm{T}} M_l^{\mathrm{b}}\xi_{l,k} \\ &-\left(\mathrm{Ad}_l^k\left(\mathrm{ad}_{\hat{\xi}_{k-1,i}}\hat{\xi}_k\right)\right)^{\vee\mathrm{T}} M_l^{\mathrm{b}}\xi_{l,j} \\ &-\left(\mathrm{Ad}_l^k\left(\mathrm{ad}_{\hat{\xi}_{k-1,j}}\hat{\xi}_k\right)\right)^{\vee\mathrm{T}} M_l^{\mathrm{b}}\xi_{l,i}\Bigg\}\end{aligned} \tag{16}$$

where the definition of Ad^i_j can be found in Appendix, $[\,\cdot\,]^{\vee\mathrm{T}} = ([\,\cdot\,]^{\vee})^{\mathrm{T}}$, and "ad" is an adjoint representation.

As a result, we obtain the following conclusions:

Conclusion 2.1. The partial result of Γ_{ijk} is presented in Table II, when $i, j, k = 1, 2, 3$.

Conclusion 2.2. Γ_{ijk} has no relationship with x^l where $l \leq \min\{\max\{i, 2\}, \max\{j, 2\}, \max\{k, 2\}\}$ according to Conclusion 1.2 and (13).

Conclusion 2.3. $\Gamma_{ijk} = 0$ when $i = 1, 2$, accordingly, Γ_{ijk} $(k \geq 4)$ is independent of x^1, x^2, and x^3.

C. Generalized Force

$Y = [Y_1, Y_2, \ldots, Y_n]^{\mathrm{T}}$ are the generalized forces in the configuration space, including the generalized forces of joint torques ${}^{\tau}Y = [{}^{\tau}Y_1, {}^{\tau}Y_2, \ldots, {}^{\tau}Y_n]^{\mathrm{T}}$ and the generalized forces of frictions ${}^{f}Y = [{}^{f}Y_1, {}^{f}Y_2, \ldots, {}^{f}Y_n]^{\mathrm{T}}$. A force can be described by the notion of a wrench as an element of $se^*(3)$ [7]. Therefore, the forces $W = [W_1, W_2, \ldots, W_n]^{\mathrm{T}}$ in the Cartesian space can be mapped into the generalized forces Y in the configuration space Q by the pull-back of the extended forward kinematics map κ^* ([8]) as

$$Y = \kappa^*\left(\sum_{i=1}^{n} W_i dy^i\right) = \sum_{j=1}^{n}\left(\sum_{i=1}^{n} W_i \left.\frac{\partial g_{s,i}}{\partial x^j}\right|_{SE(3)}\right)dx^j. \tag{17}$$

According to (17), we can calculate the generalized forces of joint torques and those of frictions respectively. The ith joint motor output a torque, whose magnitude is τ_i, and

TABLE III

RESULT OF $\partial b_{s,i}/\partial x^j$

		i					
		1	2	3	4	$\cdots$	n
	1	B	B	B	B	$\cdots$	B
	2	$0_{3\times1}$	C	C	C	$\cdots$	C
	3	$0_{3\times1}$	$0_{3\times1}$	✓	✓	$\cdots$	✓
j	4	$0_{3\times1}$	$0_{3\times1}$	$0_{3\times1}$	✓	$\cdots$	✓
	$\vdots$	$\vdots$	$\vdots$	$\vdots$	$\vdots$	$\ddots$	$\vdots$
	n	$0_{3\times1}$	$0_{3\times1}$	$0_{3\times1}$	$0_{3\times1}$	$\cdots$	✓

$B = [1,0,0]^{\mathrm{T}}$; $C = [0,1,0]^{\mathrm{T}}$; '✓' means $\partial b_{s,i}/\partial x^j \neq 0_{3\times1}$.

$\tau_1, \tau_2, \tau_3 = 0$ because of the virtual joints. Therefore, ${}^{\tau}Y_j$ can be presented as

$$ {}^{\tau}Y_j = \begin{cases} \tau_j, & \text{for } j \geq 4 \\ 0, & \text{for } j = 1,2,3. \end{cases} \tag{18}$$

Additionally, the generalized force ${}^{f}Y_j$ is computed by

$$ {}^{f}Y_j = \sum_{i=1}^{n} f_i \cdot \frac{\partial b_{s,i}}{\partial x^j}, \qquad \text{for } j = 1,\ldots,n \tag{19}$$

$$ \frac{\partial \tilde{b}_{s,i}}{\partial x^j} = \begin{cases} \hat{\xi}_{s,j}\tilde{b}_{s,i}, & \text{for } i \geq j \\ 0, & \text{for } i < j \end{cases} \tag{20}$$

where $\tilde{b}_{s,i}$ is the homogeneous vector of $b_{s,i}$, and f_i is the resultant force of the frictions acting on the ith module ($f_1 = f_2 = 0$). Generally, f_i can be further decomposed into a friction in the tangent direction and a friction in the normal direction acting on the ith module [3], [4].

By calculation, we obtain the following conclusions:

Conclusion 3.1. The result of $\partial b_{s,i}/\partial x^j$ is presented in Table III.

Conclusion 3.2. ${}^{f}Y_j$ has no relation with f_i in the case of $i < j$, according to Table III and (19).

D. Dynamics of Locomotion-manipulation

According to the above analysis, we multiply two sides of (7) by M, and trim the dynamic equation as follows:

$$ \sum_{j=1}^{n} M_{kj}\ddot{x}^j + \sum_{i=1}^{n}\sum_{j=1}^{n} \Gamma_{ijk}\dot{x}^i\dot{x}^j - {}^{f}Y_k = \tau_k \tag{21}$$

for $k = 1,\ldots,n$. Being similar to the dynamic equation of a manipulator, the first term is an acceleration-related inertia term, the second item represents a Coriolis and centrifugal term, the third term is the friction, and the right-hand side is a driving torque. Now, we unify the dynamics for locomotion and manipulation into the manipulator dynamic format.

IV. UNIFICATION OF DYNAMICS

A. Dynamics of Locomotion

The dynamics of locomotion are analyzed based on the precondition that the joint controllable angles of the snake-like robot are known. By a row-wise partitioning, (21) can be decomposed into two parts as

□ Equ1–Equ3:

$$ \begin{aligned} &\sum_{j=1}^{3} M_{kj}\ddot{x}^j + \sum_{i=1}^{3}\sum_{j=1}^{3} \Gamma_{ijk}\dot{x}^i\dot{x}^j - {}^{f}Y_k \\ &+ \left(\sum_{j=4}^{n} M_{kj}\ddot{x}^j + \sum_{i=4}^{n}\sum_{j=4}^{n} \Gamma_{ijk}\dot{x}^i\dot{x}^j \right) = 0 \end{aligned} \tag{22}$$

for $k = 1,2,3$.

□ Equ4–Equ$n$:

$$ \sum_{j=1}^{n} M_{kj}\ddot{x}^j + \sum_{i=1}^{n}\sum_{j=1}^{n} \Gamma_{ijk}\dot{x}^i\dot{x}^j - {}^{f}Y_k = \tau_k \tag{23}$$

for $k = 4,\ldots,n$.

Equation (22) describes the locomotion (x^1, x^2, x^3) of the snake-like robot, when the joint inputs $(x^4,\ldots,x^n)$ are considered as the known variables. Under the precondition, we find that 1) M_{13} and M_{23} only relate to x^3, and 2) M_{33} is known, according to Table I or Conclusion 1.2. $M_{1:3\times4:n}$ is independent of x^1 and x^2, so $M_{1:3\times4:n}$ is a function of x^3 according to Conclusion 1.2. Similarly, considering Conclusion 2.2, Γ_{ijk} $(k = 1,2,3)$ is a function of the variable x^3. Particularly, $\Gamma_{ijk} = 0$ (i or $j = 1,2$), and $\Gamma_{333} = 0$. The friction term ${}^{f}Y_k$ $(k = 1,2,3)$ is dependent on $x^i, \dot{x}^i$ $(i = 1,2,3)$. Therefore, (22) can be rewritten as

$$ \begin{aligned} &\begin{bmatrix} \sum_{i=3}^{n} m_i & 0 & M_{13}(x^3) \\ 0 & \sum_{i=3}^{n} m_i & M_{23}(x^3) \\ M_{13}(x^3) & M_{23}(x^3) & M_{33} \end{bmatrix} \begin{bmatrix} \ddot{x}^1 \\ \ddot{x}^2 \\ \ddot{x}^3 \end{bmatrix} + \begin{bmatrix} \Gamma_{331}(x^3) \\ \Gamma_{332}(x^3) \\ 0 \end{bmatrix} \dot{x}^3\dot{x}^3 \\ &- \begin{bmatrix} {}^{f}Y_1(\dot{x}^1,\dot{x}^2,\dot{x}^3,x^1,x^2,x^3) \\ {}^{f}Y_2(\dot{x}^1,\dot{x}^2,\dot{x}^3,x^1,x^2,x^3) \\ {}^{f}Y_3(\dot{x}^1,\dot{x}^2,\dot{x}^3,x^1,x^2,x^3) \end{bmatrix} + \begin{bmatrix} {}^{c}F_1(x^3) \\ {}^{c}F_2(x^3) \\ {}^{c}F_3(x^3) \end{bmatrix} = \begin{bmatrix} 0 \\ 0 \\ 0 \end{bmatrix}. \end{aligned} \tag{24}$$

We point out that the fourth term on the left hand side of (24) represents the terms in parenthesis of (22), which contain the coupled inertia, Coriolis, and centrifugal term of the joint angle movement applying at (x^1, x^2, x^3). In fact, (24) (or (22)) consists of two force equilibrium equations of the whole system in X direction and Y direction and one torque equilibrium equation of the whole system around Z direction with respect to the inertial coordinate frame. Because $|M_{1:3\times1:3}| \neq 0$, (24) is a group of ordinary differential equations with the independent variables (x^1, x^2, x^3).

Therefore, the dynamics of locomotion can been decoupled into two parts: exterior dynamics (22) (or 24) and interior dynamics (23). Given the torques of the virtual joints $\tau_1, \tau_2, \tau_3 = 0$, the accelerations ($\ddot{x}^1$, $\ddot{x}^2$, $\ddot{x}^3$) are computed from the exterior dynamic equations, which is a forward dynamics calculation. Exterior dynamics depict the locomotion of the snake-like robot in the inertial coordinate system. Correspondingly, calculating the torque τ_k $(k = 4,\ldots,n)$ in the interior dynamics equation (23) is an inverse dynamics problem. Interior dynamics describe the relationship between the body shape and the joint torques. When the snake-like robot move, exterior dynamics and interior dynamics exist at the same time and act on each other.

B. Dynamics of Manipulation

The snake-like robot can manipulate an object with its redundant body, when one end is fixed on a base. In a general way, the dynamic equations of manipulation can be derived from the dynamic equations (21) by adding the constraints ($x^1, x^2, x^3 = 0$). Consequently, each term of the dynamic equations need be recomputed with the constraints. However, this general method ignores many intrinsic dynamic characters of locomotion and manipulation. Considering the conclusions in Section III and the geometrical thought, we can directly derive the dynamic equations of manipulation from those of locomotion without recomputing each term, except the frictions.

According to Conclusion 1.2, $M_{4:n\times 4:n}$ is independent of (x^1, x^2, x^3), so $M_{4:n\times 4:n}$ is invariable in despite of any change of (x^1, x^2, x^3), even deleting the definitions of (x^1, x^2, x^3). Similarly, Γ_{ijk} $(k \geq 4)$ is also invariable when the tail is fixed, according to Conclusion 2.3. Therefore, the dynamics of manipulation can been directly written as

□ Equ$'$1–Equ$'$3:

$$\begin{bmatrix} x^1 \\ x^2 \\ x^3 \end{bmatrix} = \begin{bmatrix} 0 \\ 0 \\ 0 \end{bmatrix} \tag{25}$$

□ Equ$'$4–Equ$'n$:

$$\sum_{j=4}^{n} M_{kj}\ddot{x}^j + \sum_{i=4}^{n}\sum_{j=4}^{n}\Gamma_{ijk}\dot{x}^i\dot{x}^j - {}^fY'_k = \tau_k \tag{26}$$

for $k = 4, \ldots, n$. Therein, ${}^fY'_k$ is the generalized force of the frictions applying at x^k in manipulation.

Equation (25) means that the tail of the snake-like robot is fixed. Naturally, (26) implies the dynamics of the manipulator, which is proven in the following way. In Section II, the configuration of the snake-like robot in the manipulation state is $x' \in Q'$, and the configuration of the manipulator is $x'' \in N$. According to the Gauss equations in Riemannian manifold, we can obtain the following equation

$$\nabla'_{\dot{x}'}\dot{x}'\,\big|_{\alpha(N)} = \nabla''_{\dot{x}''}\dot{x}'' + B(\dot{x}'', \dot{x}'') \tag{27}$$

where ∇' and ∇'' are the Levi-Civita connections in Q' and N respectively, $B(x'', x'') \in T^{\perp}N$, and $T^{\perp}N$ is the normal bundle of N in TQ'. Because of the fixation of one end, the normal space of N at a point x'' in TQ' becomes $T^{\perp}_{x''}N = 0$, so that $B(\dot{x}'', \dot{x}'') = 0$. Therefore,

$$\nabla'_{\dot{x}'}\dot{x}'\,\big|_{\alpha(N)} = \nabla''_{\dot{x}''}\dot{x}''. \tag{28}$$

Completely, we can safely conclude that (26) is the dynamic equation of the manipulator.

With the unification of dynamics, a map β^* induces the metric tensor M on Q to the metric tensor M_A on N. Thus, the metric matrix of the manipulator is the sub-matrix of the metric matrix of the snake-like robot. In addition, the property of Γ_{ijk} in Conclusion 2.1-2.3 is crucial to the unification as well. Because of the two aspects, the dynamic equations of the manipulator can be directly degenerated from those of the snake-like robot.

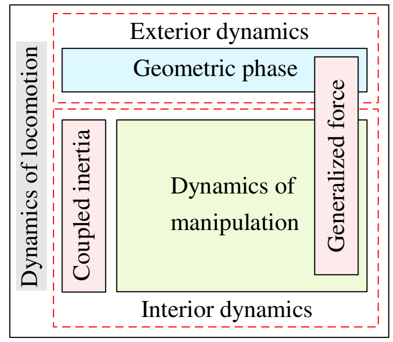

Fig. 3. Dynamic relationship for locomotion and manipulation of the snake-like robot

The frictions, which are the interactions between the snake-like robot and the environment, cannot be unified. However, ${}^fY'_k$ can be directly computed from ${}^fY_k$ due to Conclusion 3.2 and the property of POE. Therefore,

$${}^fY'_k = {}^fY_k(x^1 = 0, x^2 = 0, x^3 = 0), \quad \text{for } k = 4, \ldots, n.$$

C. Expatiation for Unification

The dynamics of the snake-like robot include exterior dynamics and interior dynamics. When one end is fixed, exterior dynamics degenerate into zeros; and interior dynamics become into the dynamics of the manipulator. The unified dynamic model of locomotion-manipulation is established, and the relationship of the model is shown in Fig. 3. Additionally, the unification also reveals the particular structure of the dynamic model of the snake-like robot.

The unification of dynamics can be simply realized because of the following reasons: First, VSOP unifies the snake-like robot and the manipulator in mechanism. Second, POE is suitable to represent the unification in kinematics. Third, the Lie group formulation receives the computationally effective equations. Finally, the dynamic equation in manifold provides a geometrical point of view in comprehending the dynamics of locomotion-manipulation. In fact, the dynamic problems of the snake-like robot are considered as submanifold problems by comparing with those of the manipulator. In addition, the geometric relationship between the dynamic equations of locomotion and those of manipulation can be described as induced connection (27). Other methods, such as [4], [5], can hardly establish and prove the uniform dynamic relationship without the geometrical tool.

V. Numerical Simulation

Hirose used the serpenoid curve to generate the gaits of the snake-like robot [1]. Practically, the curve can be realized by controlling the relative joint angles as

$$x^i(t) = \alpha \sin(\omega t + (i-3)\beta) + \gamma, \quad \text{for } i = 4, \ldots, n \tag{29}$$

where α, β, and γ determine the shape of the robot, and ω represents the speed of undulation [4]. For the convenience of comparison, (29) is used to control both locomotion

TABLE IV

PARAMETERS OF SIMULATION

Number of real units	5	α	$0.4\,\mathrm{rad}$	Tangential Coulomb friction coefficient	0.01
Length of unit	$0.08\,\mathrm{m}$	ω	$1\,\mathrm{rad/s}$		
Mass of unit	$0.5\,\mathrm{kg}$	β	$0.5\pi\,\mathrm{rad}$	Normal Coulomb friction coefficient	0.50
Inertia of unit	$0.016\,\mathrm{kg{\cdot}m^2}$	γ	$0\,\mathrm{rad}$		

Let each real unit be of the same length, mass, and inertia respectively.

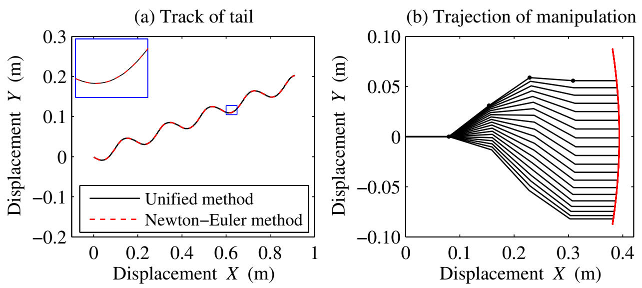

Fig. 4. (a) Track of the tail in the locomotion-manipulation method comparing with that in the Newton-Euler method. Partial enlargement zoomed the displacement $X \in [0.60, 0.65]$ is drawn proportionally. (b) Trajectory of manipulation controlling by the serpenoid curve.

and manipulation of the snake-like robot which consists of five real modules with passive wheels. Additionally, the Coulomb friction model is used to describe the interaction between the robot and the environment in the tangent and normal direction. The dynamic equations in the locomotion-manipulation method are composed of the unified equations. For comparison, the Newton-Euler method is also used to model the dynamics of the two states respectively. The basic simulation parameters are shown in Table IV.

The tail track of locomotion and the trajectory of manipulation are depicted in Fig. 4. The torques of locomotion and manipulation comparing with those in the Newton-Euler method are presented in Fig. 5 and 6 respectively. The simulation results in our method are identical with those in the Newton-Euler method well. Comparing Fig. 5 and 6 with enlargement, the numerical results in manipulation are more precise than those in locomotion, because the dynamics of locomotion, including interior dynamics and exterior dynamics, are more complicated than those of manipulation, including only interior dynamics.

VI. CONCLUSION

A unified dynamic model of locomotion-manipulation of the snake-like robot has been established by using differential geometry. Analysis and simulation showed its validity. Finally, we point out that 1) because the basic formulae are compatible with not only 2-D motion but also 3-D motion, so it can be extended from 2-D to 3-D; 2) the interaction force from the manipulated object is ignored in this paper.

APPENDIX

Definition ([10]). Given $A_1, \ldots, A_n \in se(3)$ and $x^1, \ldots, x^n \in \mathbb{R}$, define the map $\mathrm{Ad}_j^i : se(3) \to se(3)$ by

$$Ad_j^i(H) = \begin{cases} e^{-A_j x^j} \cdots e^{-A_i x^i} H e^{A_i x^i} \cdots e^{A_j x^j}, & \text{for } i \le j \\ H, & \text{for } i > j. \end{cases}$$

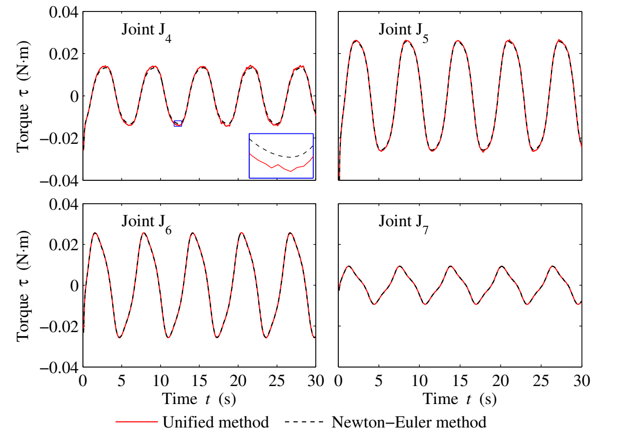

Fig. 5. Torque comparison of locomotion. Each subfigure describes the torque τ_k of locomotion at the joint J_k in the locomotion-manipulation method and that in the Newton-Euler method together ($k = 4, \ldots, 7$). Numerical error is accumulated at τ_4 most, and the average error of τ_4 is 6.09%. Partial enlargement zoomed time $t \in [11.75, 12.75]$ is drawn.

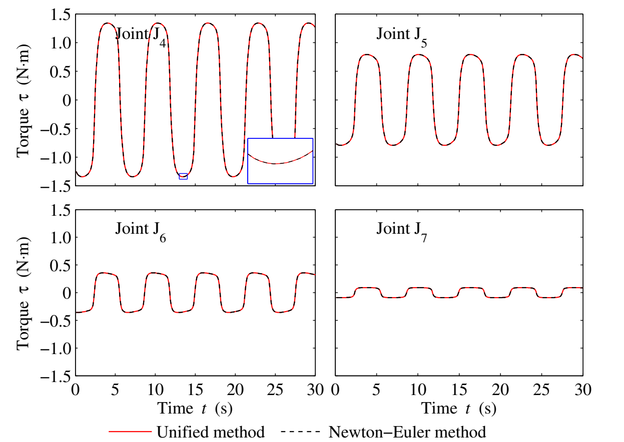

Fig. 6. Torque comparison of manipulation. Each subfigure describes the torque τ_k of manipulation in the locomotion-manipulation method and that in the Newton-Euler method ($k = 4, \ldots, 7$). Numerical error of τ_4 is 0 approximately, and partial enlargement zoomed time $t \in [13, 14]$ is drawn.

REFERENCES

[1] S. Hirose, *Biologically Inspired Robots (Snake-like Locomotor and Manipulator)*. Oxford, U.K.: Oxford University Press, 1993.

[2] J. Ostrowski and J. Burdick, "Gait kinematics for a serpentine robot," in *Proc. IEEE Int. Conf. Robot. Autom.*, vol. 2, Minneapolis, Apr. 1996, pp. 1294–1299.

[3] S. Ma, "Analysis of creeping locomotion of a snake-like robot," *Adv. Robot.*, vol. 15, pp. 205–224, 2001.

[4] M. Saito, M. Fukaya, and T. Iwasaki, "Serpentine locomotion with robotic snakes," *IEEE Control Syst. Mag.*, vol. 22, no. 1, pp. 64–81, 2002.

[5] P. Liljebäck, Ø. Stavdahl, and K. Y. Pettersen, "Modular pneumatic snake robot: 3D modelling, implementation and control," *Proc. 16th IFAC World Congr.*, Jul. 2005.

[6] S. B. Andersson, "Discretization of a continuous curve," *IEEE Trans. Robot.*, vol. 24, no. 2, pp. 456–461, 2008.

[7] R. M. Murray, Z. Li, and S. S. Sastry, *A Mathematical Introduction to Robotic Manipulation*. Florida: CRC Press, 1994.

[8] M. Žefran and F. Bullo, "Lagrangian dynamics," in *Robotics and Automation Handbook*, T. R. Kurfess, Ed. Florida: CRC Press, 2005.

[9] T. Frankel, *The Geometry of Physics: An Introduction*, 2nd ed. Cambridge, U.K.: Cambridge University Press, 2004.

[10] F. C. Park, J. E. Bobrow, and S. R. Ploen, "A lie group formulation of robot dynamics," *Int. J. Rob. Res.*, vol. 14, no. 6, pp. 609–618, 1995.